PPPL-2036 I-11550 PPPL-2036

UC20-G

PPPL--2036

DE84 000906

HELIAC PARAMETER STUDY

By

D.A. Monticello, R.L. Dewar, H.P. Furth, and A. Reiman

September 1983

PLASMA PHYSICS LABORATORY

PPL

PRINCETON UNIVERSITY

PRINCETON, NEW JERSEY

PREPARED FOR THE U.S. DEPARTMENT OF ENERGY, UNDER CONTRACT DE-AC02-76-CHO-3073.

HELIAC PARAMETER STUDY

D. A. Monticello, R. L. Dewar,* H. P. Furth, and A. Reiman

Plasma Physics Laboratory, Princeton University

Princeton, New Jersey 08544

ABSTRACT

Helical axis stellarators (heliacs) with zero net current are found to possess very good stability properties. Helically symmetric or "straight" heliacs with bean-shaped cross sections have a first region of stability that reaches to $\langle\beta\rangle$ of 30% or more. Those with circular cross sections have a second region of stability to Mercier modes. In addition we report on the stability properties of these plasma configurations as functions of pressure profile, helical aspect ratio, and helical period length.

*Permanent address: Department of Theoretical Physics, Research School of Physical Sciences, The Australian National University, Canberra, Australia.

I. INTRODUCTION

The superposition of an $\ell = 1$ stellarator field on the tokamaklike field of a current carrying toroidal conductor and a solenoid field produces nested helical flux surfaces of bean-shaped minor cross sections. The strongly helical curvature of the magnetic axis lends itself to the realization of a deep magnetic well, even in the large aspect ratio limit.[1,2] Thus these heliac configurations do not have to rely on toroidal curvature to provide a magnetic well as do planar axis stellarators. We restrict ourselves here to the study of helically symmetric heliacs. These "straight" heliacs should give good quantitative agreement with toroidal heliacs when the toroidal curvature is large (i.e., when the number of helical periods is much greater than one). We have previously reported on the favorable finite beta stability of these configurations.[3] We here report on further studies of this configuration and on the stability of other helical axis configurations that do not have a well at zero beta. These have more nearly circular cross sections and can be produced with very simple coils.[4] The stability of these configurations is studied as functions of the pressure profile, helical aspect ratio, and helical period length. In Sec. II we describe the heliac equilibria and their parameterization. In Sec. III the stability of these equilibria is described and Sec. IV contains a discussion of the magnetic axis shift as a function of beta.

II. EQUILIBRIA

A three-dimensional view of the helically symmetric magnetic surfaces that we will be calculating is shown in Fig. 1 in an r, ϕ, z coordinate system. All equilibrium quantities are assumed to be functions only of r and u, where

$$u = \phi - hz \quad , \tag{1}$$

with

$$h = \frac{2\pi}{L} \quad . \tag{2}$$

Here, L is the length in the z direction of the length of one helical period. With this assumed symmetry the magnetic field can be represented as

$$\underset{\sim}{B} = h\underset{\sim}{u} \times \underset{\sim}{\nabla}\psi + hg\underset{\sim}{u} \quad , \tag{3}$$

where

$$\underset{\sim}{u} = \frac{\hat{z} + hr\hat{\phi}}{1 + h^2r^2} \quad . \tag{4}$$

The equilibrium equation $J \times B = \nabla P$ then becomes

$$\underset{\sim}{\nabla} \cdot \left(K \underset{\sim}{\nabla}\psi\right) = -\frac{2k^2}{h} g - kg \frac{\partial g}{\partial \psi} - \frac{\partial p}{\partial \psi} \quad , \tag{5}$$

where

$$K = \frac{h^2}{1 + h^2r^2} \quad . \tag{6}$$

The equilibrium is determined by specifying the shape of the outer flux surface (where $\partial p/\partial \psi = 0$) in a z = constant plane. The parameterization is

$$x = \rho \cos\gamma + \bar{x} \quad , \tag{7}$$

$$y = \rho \sin\gamma \quad , \tag{8}$$

where

$$\gamma = B \sin(\pi - \theta) \quad , \tag{9}$$

$$\rho = a[1 - b \cos(\pi - \theta)] \quad . \tag{10}$$

Shown in Fig. 2 is the z = constant cross section that we will use as our reference heliac. It has

$$a = 0.5, \quad b = 0.5, \quad \bar{x} = 0.2 \quad , \tag{11}$$

and values of B from 0.6 to 1.6. Figure 3 shows the cross section for two different values of the helical aspect ratio A. Here the parameters are

$$a = 0.5, \quad b = 0.5, \quad \bar{x} = 0.2, \quad \text{and } \bar{x} = 0.4, \tag{12}$$

and

$$B = 1.6 \quad . \tag{13}$$

The pressure $p(\psi)$ is parameterized as $p = c\psi^{\alpha}$ and representative profiles are shown in Fig. 4. We note that the ratio of the area averaged pressure to the on-axis pressure is 0.4, 0.33, and 0.25 for α equal to 2, 3, and 4,

respectively.

Finally, the function $g(\psi)$ is chosen to make the net toroidal (z-direction) current through each flux surface vanish. This constraint implies that there is no ohmic heating current, and if the conductivity is constant on a flux surface, that the equilibria are true resistive equilibria.

A description of the flux coordinate equilibrium code FEQ2.5 that solves Eq. (5) subject to this constraint is contained in Ref. 5. Figure 5 shows typical results from this code for the vacuum field transforms of the reference heliac case with B = 1.6 and 1.2. Figure 6 shows the transforms for $\langle\beta\rangle$ of approximately 20% for the same cases.

III. STABILITY

We present in this section the balloon and Mercier stability of the equilibria described above. The formulation for this calculation is contained in Ref. 5 along with a discussion of the global stability analysis, the results of which we also briefly mention.

Figure 6 is the stability diagram for the reference case. There are three regimes indicated in Fig. 6. A stable region that exists for large B, a region where both balloon and Mercier criterion give instability, and a region where just the balloon criterion gives instability. At low β the $V'' < 0$ condition[7] for stability is seen to be consistent with the balloon and Mercier criteria as it should be. A characteristic of the equilibria described here is that when $V'' = 0$ vanishes at the origin, it is approximately zero over the whole cross section of the plasma. Figure 6 shows cases with $\langle\beta\rangle > 30\%$ for B = 1.6 that are stable. Here $\langle\beta\rangle$ is defined relative to the vacuum field on axis. These have on-axis beta values (relative to local B) of ≈200% because of the diamagnetic effect of the plasma. This is very desirable from the

point of view of advanced fuel cycles and also would mean improved transport properties because of μ (magnetic moment) conservation. Some of these very high-β cases have been checked for global stability and no low-n modes were found (n is the helical mode number). Results similar to this have been reported by others.[6] The boundary at high β for the Mercier criterion may be viewed as a second region of stability. This is due to the fact that the critical n is typically $\gtrsim$20 for the region where the system is just ballooning unstable, whereas inside the region where the Mercier criterion is violated low-n modes are found to be very unstable. This second region of stability to the Mercier criterion has been reported elsewhere.[7] However, the region of balloon instability and Mercier stability was not included in Ref. 7. Figures 7 and 8 show the flux and current contours for a near circular plasma in this second region of stability to the Mercier criterion.

Also illustrated in the stability diagram is the ad hoc equilibrium limit.[7] This is a limit that is violated when the magnetic axis is half way between the wall and the zero beta magnetic axis position (see Sec. IV). Figure 6 shows that this limit is also favorably affected by having a more "beany" shape to the outer flux surface.

Next, Fig. 9 illustrates the effect of peaking the pressure profile. The V" boundary is of course unaffected. There is also very little effect on the balloon boundary but the Mercier boundary is improved by peaking the pressure profile. The ad hoc equilibrium-β limit is decreased as might be expected.

Figure 10 shows the effect of decreasing the length of a helical period, which is favorable for the near circular plasma but generally has a deleterious effect on the bean-shaped plasma.

Finally, Fig. 11 shows the favorable effect of large aspect ratio (except on the equilibrium limit).

IV. DISCUSSION OF EQUILIBRIUM LIMIT

In planar axis stellarators the equilibrium beta limit is believed to be due to the symmetry breaking nature of the Shafranov shift, which presumably leads to destruction of the flux surfaces. It is not known at what value of the shift the flux surfaces will be destroyed. The convention is to take the equilibrium beta limit to be that value of beta at which the magnetic axis shifts half way out to the outer flux surface. This rough estimate gives a basis for comparison of different planar axis stellarator configurations.

For the helical equilibria considered in this paper, the axis shift is purely helical and does not break the symmetry. There is, in principle, no equilibrium beta limit. In practice, however, a large helical shift will couple with the symmetry breaking corrections to the equilibrium (such as the toroidal shift, the field ripple on axis, etc.). The resulting resonant perturbations are again expected to destroy the flux surfaces. As a convenient measure of this effect, we have adopted the convention that the ad hoc equilibrium limit corresponds to the β value at which the axis shifts half way to the wall.

For nearly circular flux surfaces, the magnetic axis shift at low β is approximately given by [8,9]

$$\Delta R/r_p = \frac{1}{2} \langle\beta\rangle A/\iota_h^2 \quad , \tag{15}$$

where ι_h, the transform in the helical reference frame, is

$$\iota_h = 1 - \iota \quad , \tag{16}$$

with ι the rotational transform per period. In Fig. 13 we have plotted the axis shift as a function of the right-hand side of Eq. (15) for some of our equilibria. We see that Eq. (15) gives a reasonable approximation to the axis shifts for $B = 1.0$, even though the flux surfaces are far from circular. The axis shifts are smaller for $B = 1.2$. The linear dependence of the axis shifts on β shows that the low-β expansion used to derive Eq. (15) retains its validity even at relatively large values of the shift.

V. CONCLUSION

We have shown that the stability to Mercier and ballooning modes is very dependent on the shape of the outer flux surface and, as might be expected, this is connected closely with the existence of a well ($V'' < 0$) at zero beta. The bean-shaped heliacs have ideal stability limits that are quite high and which increase with large aspect ratio, and long helical period length. On the other hand, the more circular cross-sectional heliac is troubled at low β with low-n instability but has a second region of stability to these modes that is optimized by large helical aspect ratio, highly peaked pressure, and small helical period length.

ACKNOWLEDGMENT

This work was supported by U. S. Department of Energy Contract No. DE-AC02-76-CHO-3073.

REFERENCES

[1]H. P. Furth, J. Killeen, M. N. Rosenbluth, and B. Coppi in Plasma Physics and Controlled Nuclear Fusion Research (IAEA, Vienna, 1966), Vol. I, p. 103.

[2]B. McNamara, K. J. Whiteman, and J. B. Taylor in Plasma Physics and Controlled Nuclear Fusion Research (IAEA, Vienna, 1966), Vol. I, p. 145.

[3]A. H. Boozer, T. K. Chu, R. L. Dewar, H. P. Furth, J. A. Goree, J. L. Johnson, R. M. Kulsrud, D. A. Monticello, G. Kuo-Petravic, G. V. Sheffield, S. Yoshikawa, and O. Betancourt in Plasma Physics and Controlled Nuclear Fusion Research (IAEA, Vienna, 1983), Vol. II.

[4]A. Reiman and A. H. Boozer, Princeton Plasma Physics Laboratory Report No. PPPL-2025, 1983.

[5]R. L. Dewar, D. A. Monticello, and W. N.-C. Sy, Princeton Plasma Physics Laboratory Report No. PPPL-2027, 1983.

[6]R. Gruber, W. Kerner. P. Merkel, J. Nührenberg, W. Schneider, and F. Troyon, Comput. Phys. Commun. 24, 389 (1981).

[7]V. D. Shafranov, Phys. Fluids 26, 357 (1983).

[8]Solov'ev and Shafranov in Reviews of Plasma Physics, edited by M. A. Leontovich (Consultants Bureau, New York, 1970), Vol. 5, p. 1.

[9]A. H. Boozer, Princeton Plasma Physics Report No. PPPL-1973, 1983.

FIGURE CAPTIONS

FIG. 1. Typical helically symmetric magnetic surface ψ-constant for bean-shaped heliac in r, ϕ, z coordinate.

FIG. 2. z = constant cross section of outer flux surface for the reference heliac a = 0.5, b = 0.5, $\bar{x}$ = 0.2, and B = 0.6 to 1.6.

FIG. 3. z = constant cross section for helical aspect ratio A = 2.8 and A = 3.9.

FIG. 4. Pressure profiles as functions of distance along midplane for low-β reference heliac case with B = 1.6. (r = 0 is magnetic axis and r = r_p is edge of plasma.)

FIG. 5. Rotational transform per heliac period as a function of distance along midplane for two reference heliacs, B = 1.6 and B = 1.2 where β = 0%.

FIG. 6. Same as Fig. 5 except β is now 20%.

FIG. 7. Stability diagram for reference heliac case. NOTE: Second region of stability to Mercier modes (B = 0.6) and first region of stability to $\langle\beta\rangle$ = 30% (B = 1.6). The ad hoc equilibrium limit curve shows the ad hoc equilibrium-β limit, where the magnetic axis has shifted halfway to the wall.

FIG. 8. Magnetic surfaces of reference heliac in second region of stability (B = 0.6).

FIG. 9. Contours of current density for reference heliac in second region of stability (B = 0.6).

FIG. 10. Stability diagram for heliac showing effect of peaking the pressure (dotted curve).

FIG. 11. Stability diagram for heliac showing effect of decreasing the length of a helical period (dotted curve).

FIG. 12. Stability diagram for heliac showing effect of increasing helical aspect ratio (dotted curve).

FIG. 13. Axis shift as a function of β for several different sets of parameters. Here δ is the axis shift relative to r_p, and r_o is the radius of the magnetic axis. The solid line is the prediction of Eq. (15). The parameters considered are:

x $\alpha = 2.0$, $h = 0.8$, $A = 2.8$, $B = 1.0$

Δ $\alpha = 3.0$, $h = 0.8$, $A = 2.8$, $B = 1.0$

● $\alpha = 2.0$, $h = 0.8$ $A = 3.6$, $B = 1.0$

$= 2.0$, $h = 1.6$, $A = 2,8$, $B = 1.0$

$= 2.0$, $h = 0.8$, $A = 2.8$, $B = 1.2$

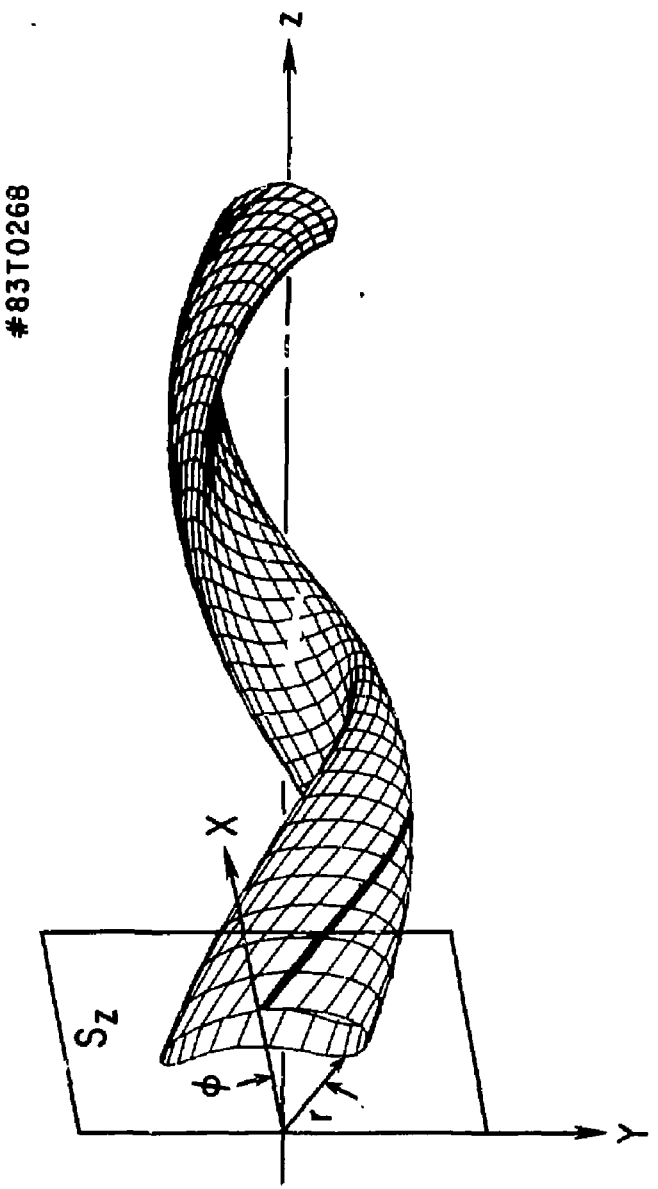

Fig. 1

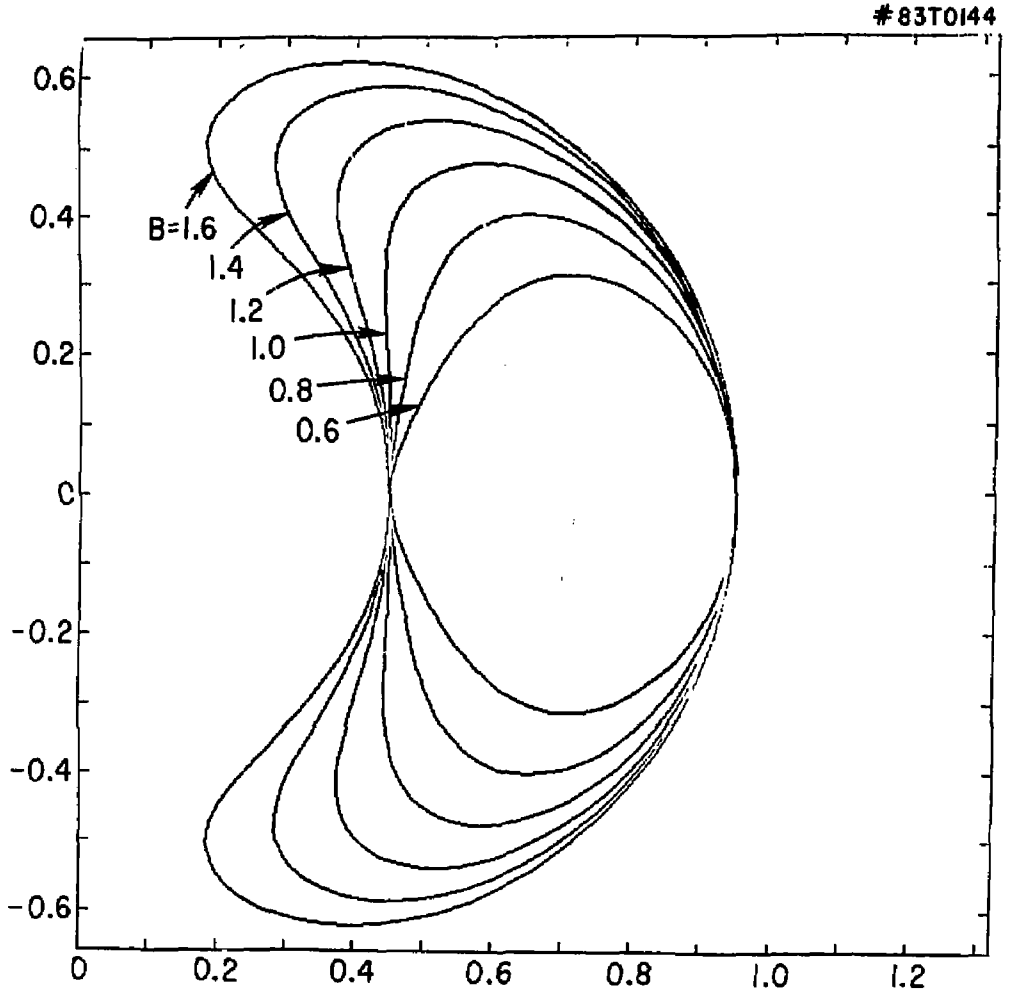

Fig. 2

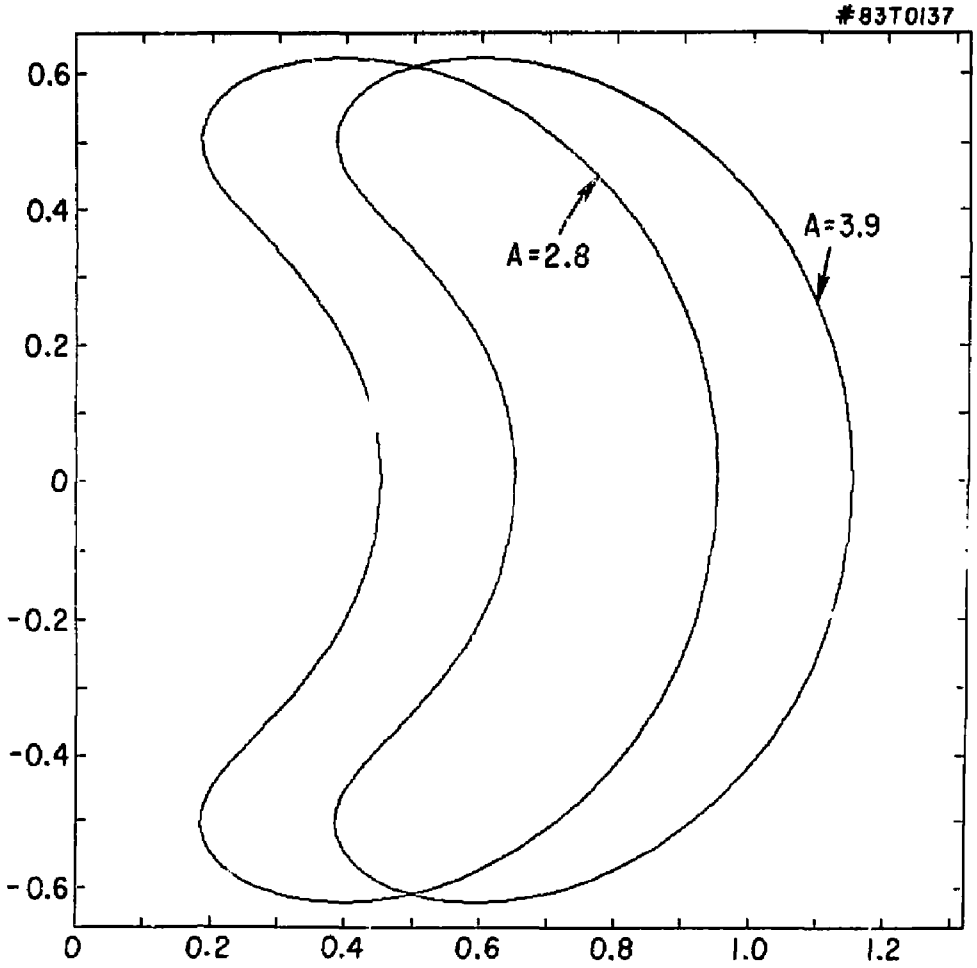

Fig. 3

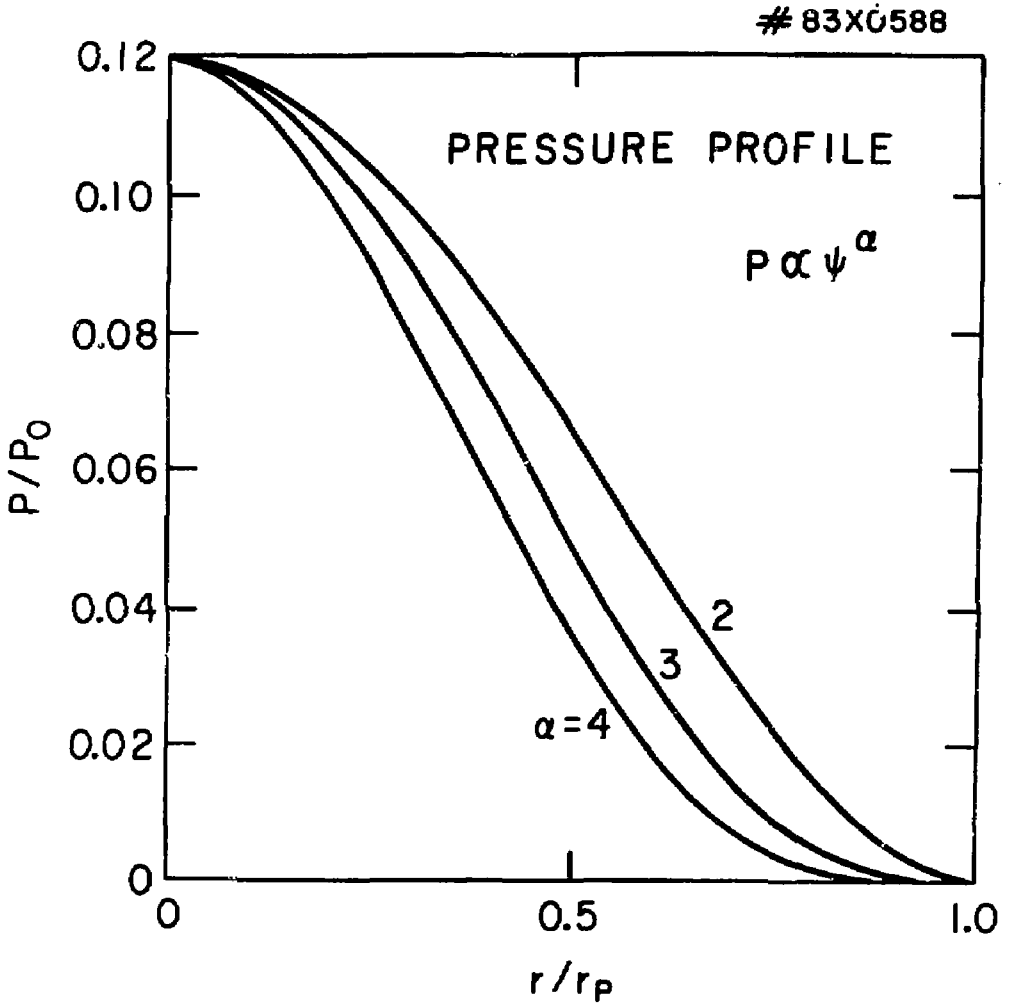
#83X0588
PRESSURE PROFILE
$P \propto \psi^{\alpha}$
0.12
0.10
0.08
0.06
0.04
0.02
0
P/P_0
2
3
$\alpha=4$
0
0.5
1.0
r/r_p

Fig. 4

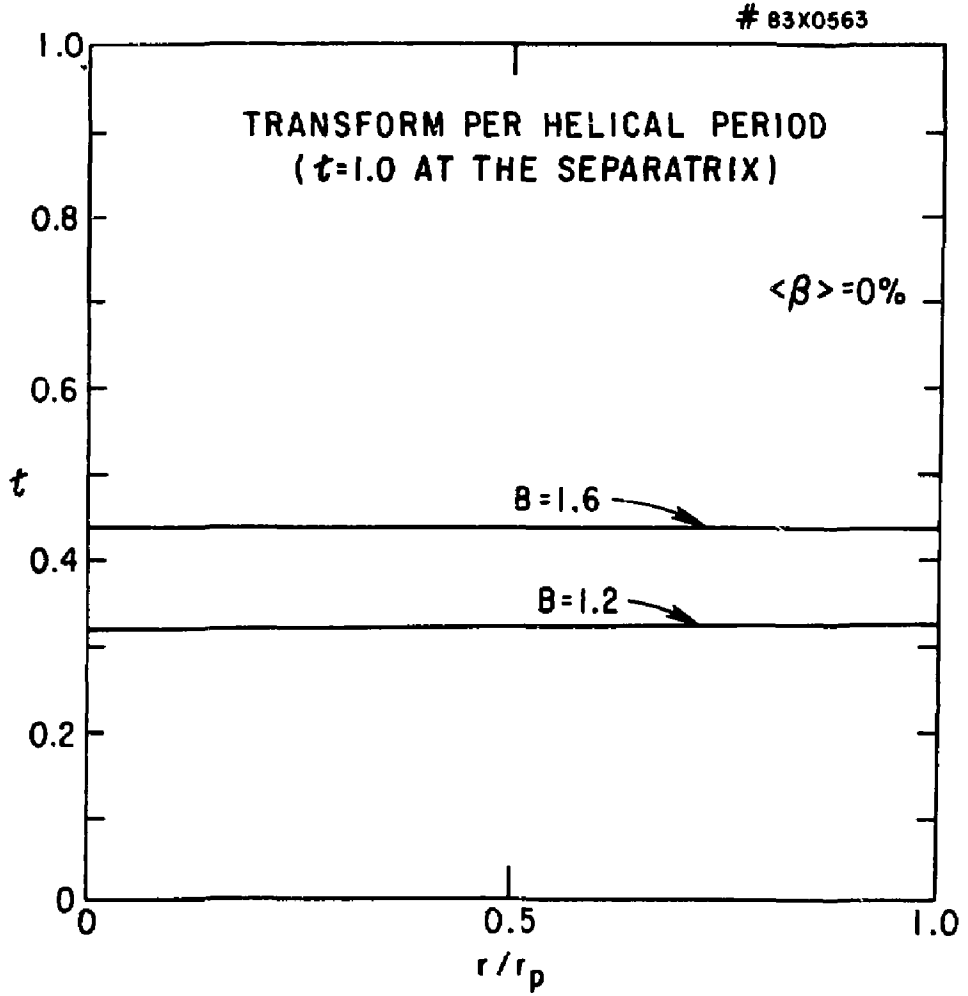
83X0563
TRANSFORM PER HELICAL PERIOD
(t=1.0 AT THE SEPARATRIX)
<β>=0%
B=1.6
B=1.2
t
r/r_p
1.0
0.8
0.6
0.4
0.2
0
0
0.5
1.0

Fig. 5

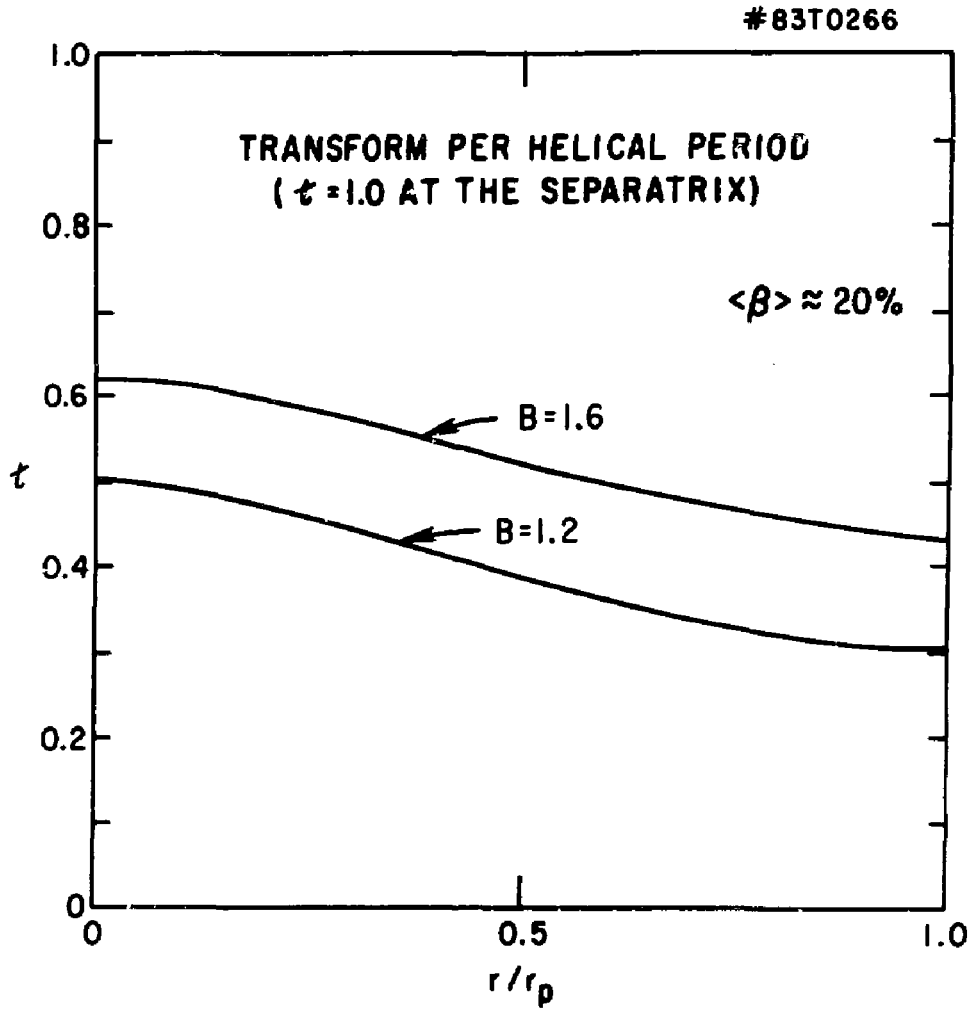
#83T0266
TRANSFORM PER HELICAL PERIOD
(t = 1.0 AT THE SEPARATRIX)
<β> ≈ 20%
B=1.6
B=1.2
t
1.0
0.8
0.6
0.4
0.2
0
0
0.5
1.0
r/rp

Fig. 6

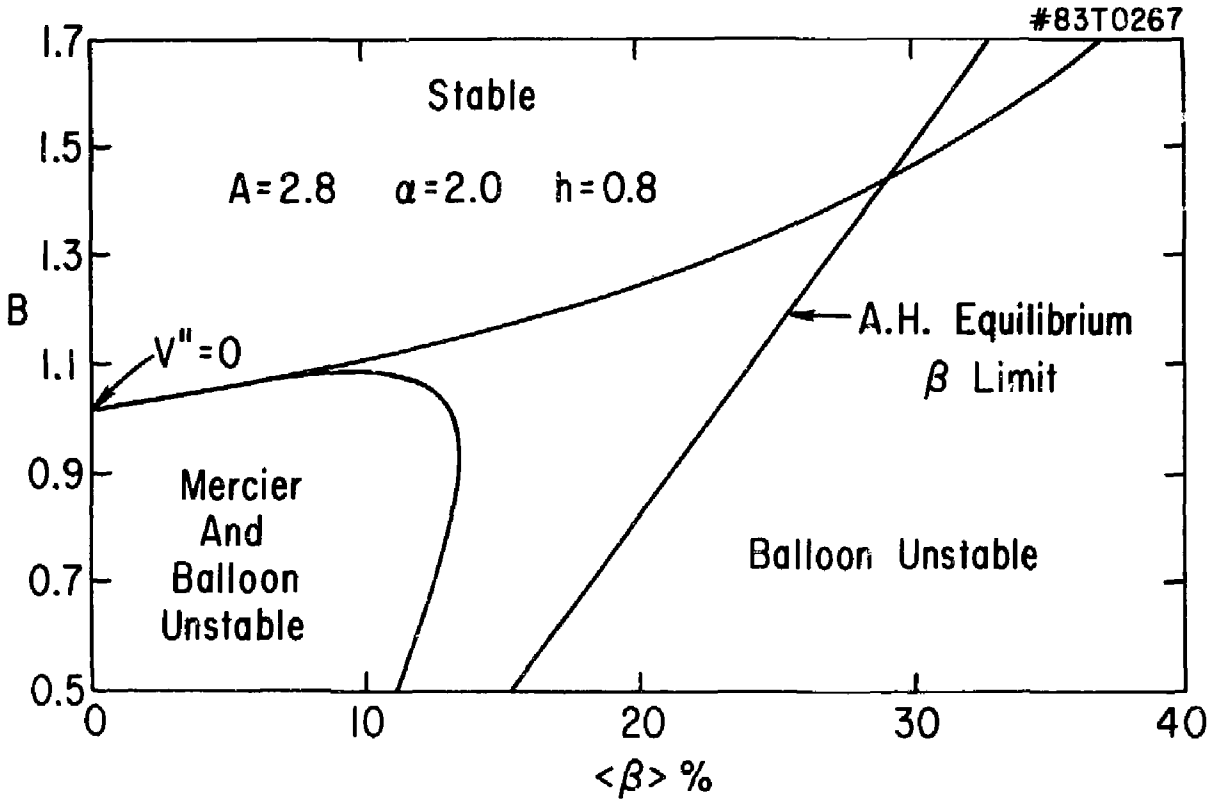
#83T0267
Stable
A=2.8 α=2.0 h=0.8
V"=0
A.H. Equilibrium
β Limit
Mercier
And
Balloon
Unstable
Balloon Unstable
B
<β> %
1.7
1.5
1.3
1.1
0.9
0.7
0.5
0
10
20
30
40

Fig. 7

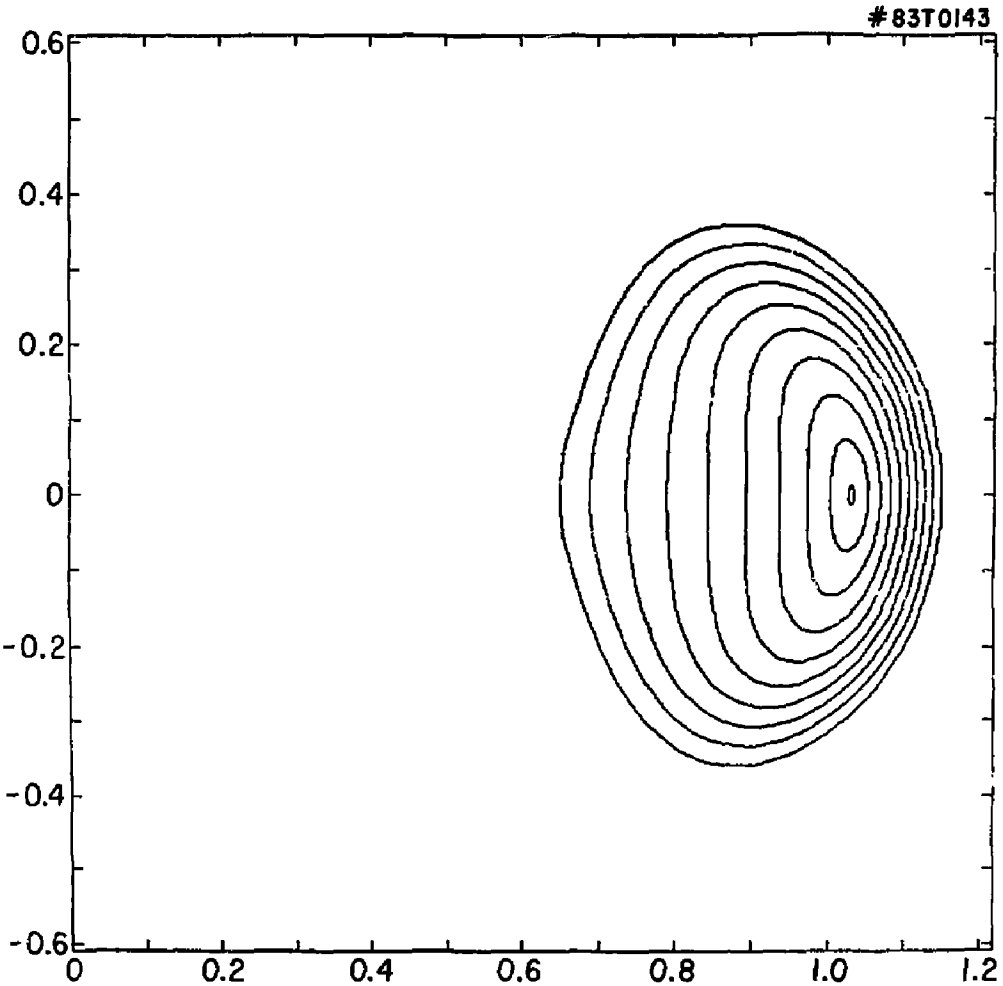

Fig. 8

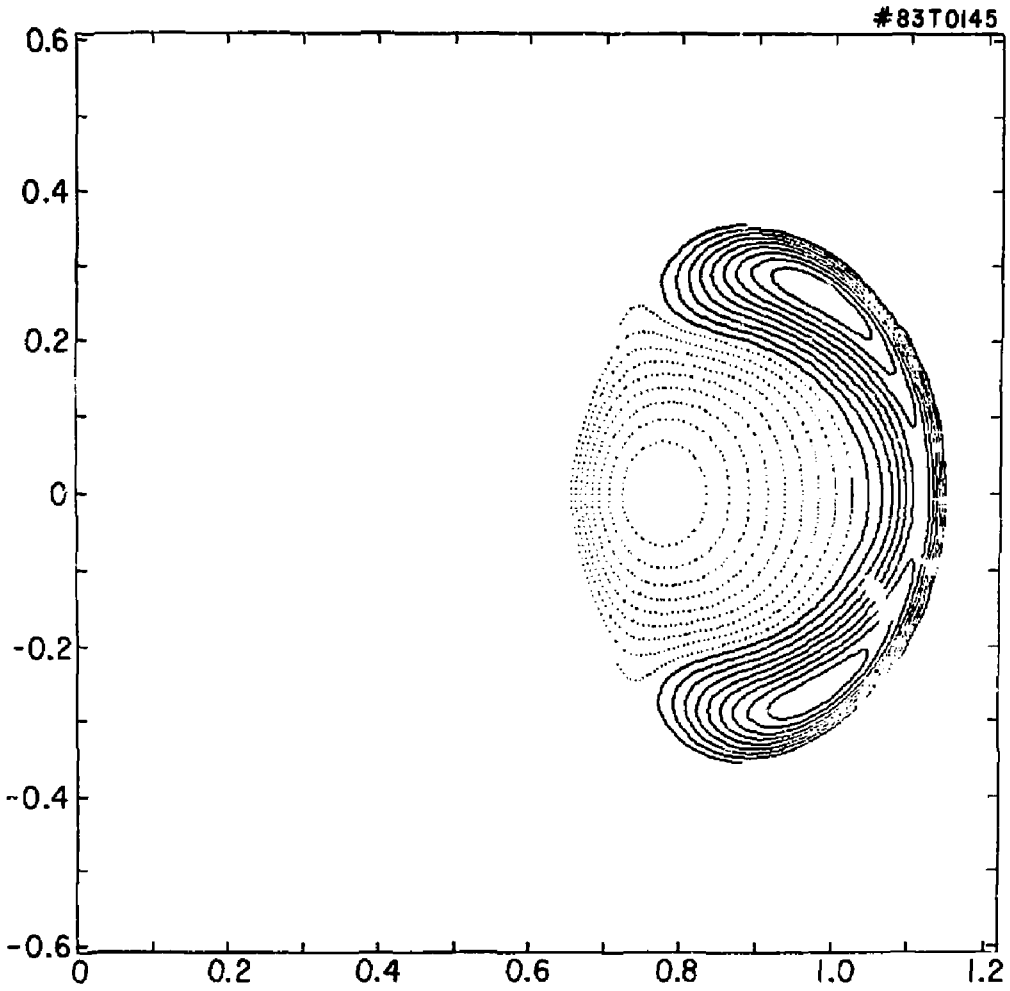

Fig. 9

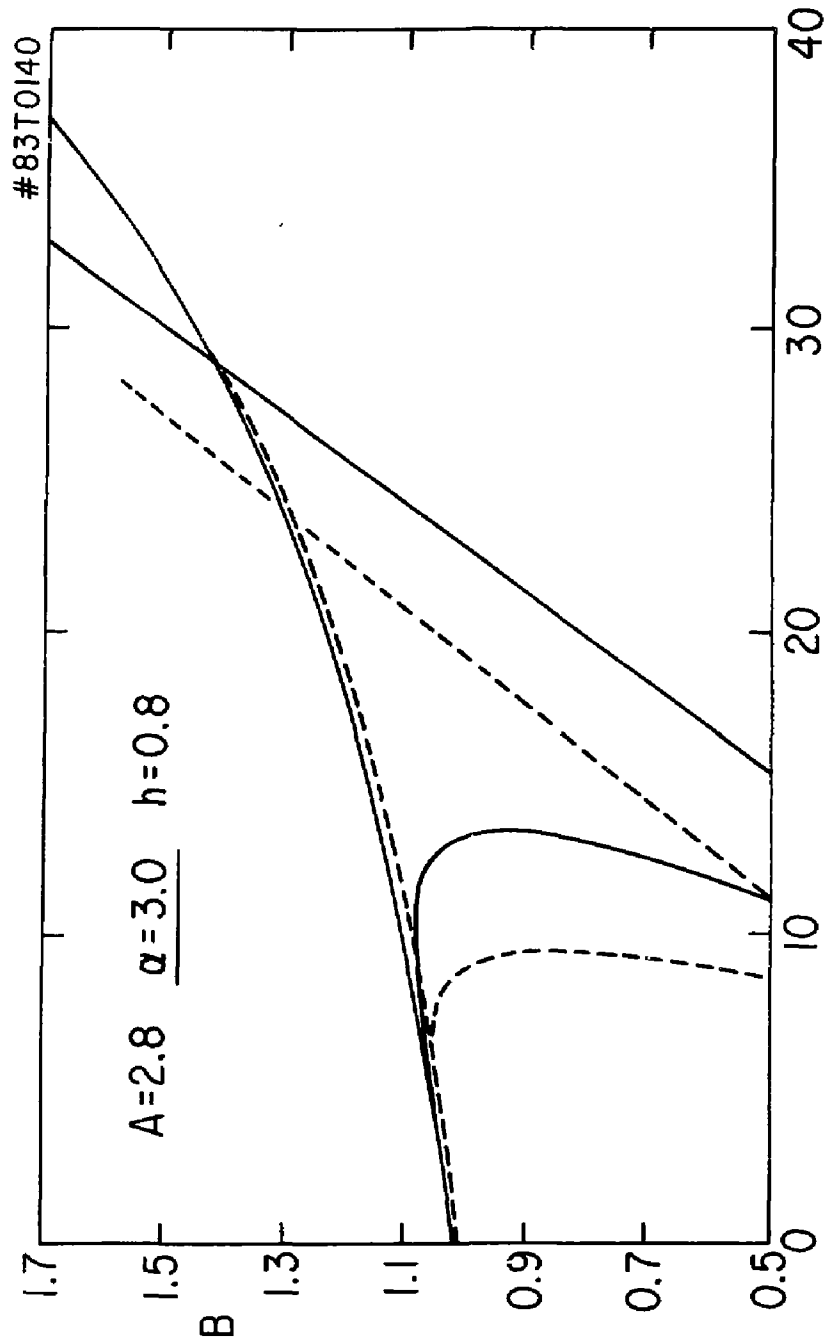

Fig. 10

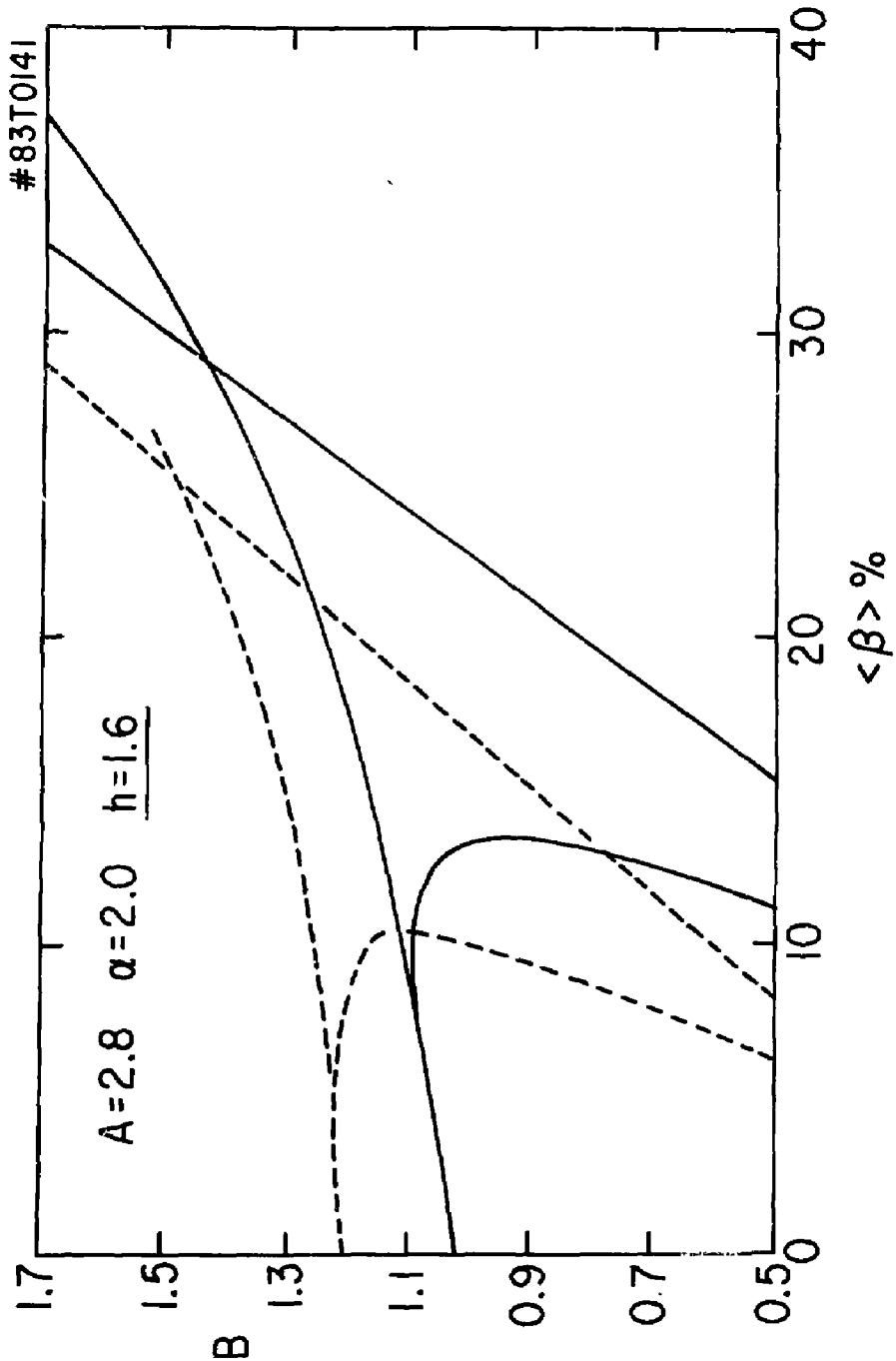

Fig. 11

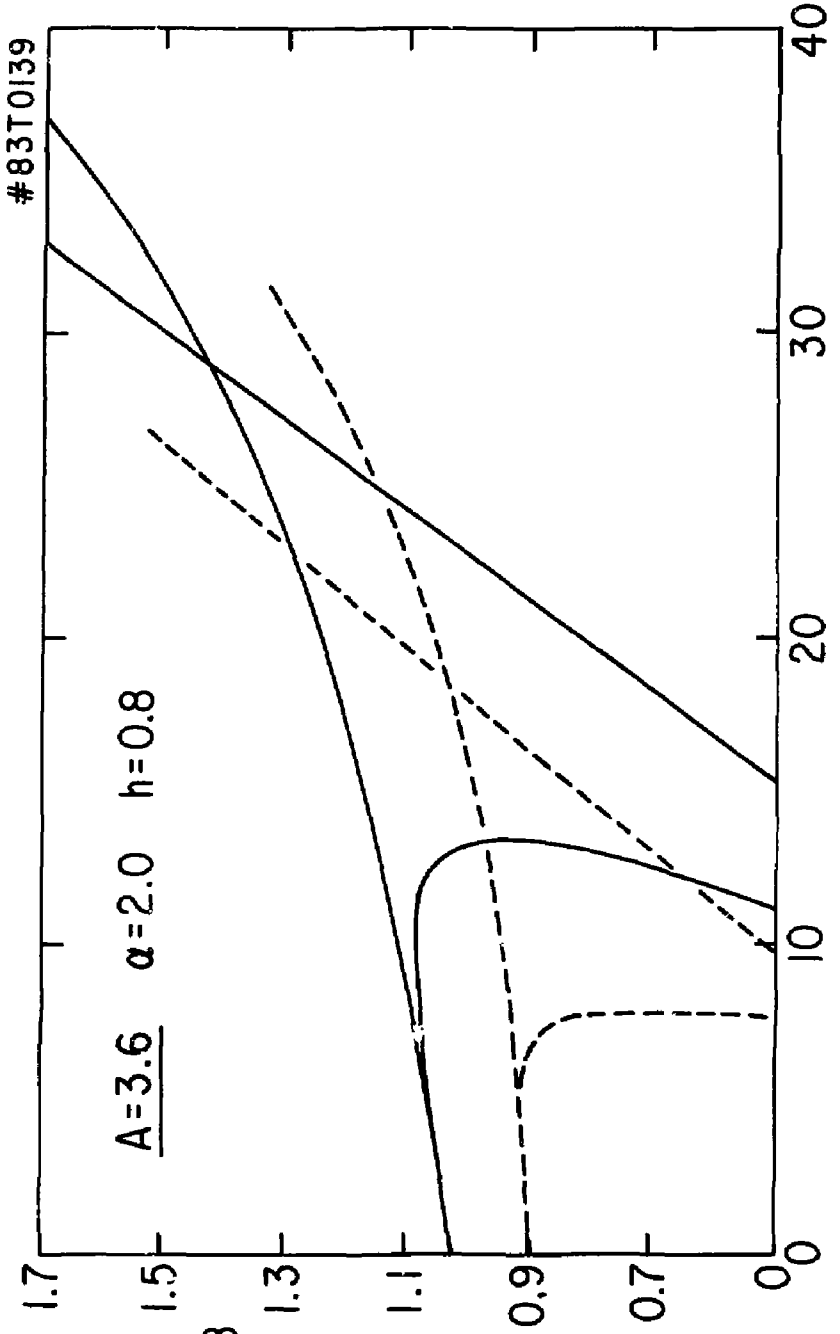

Fig. 12

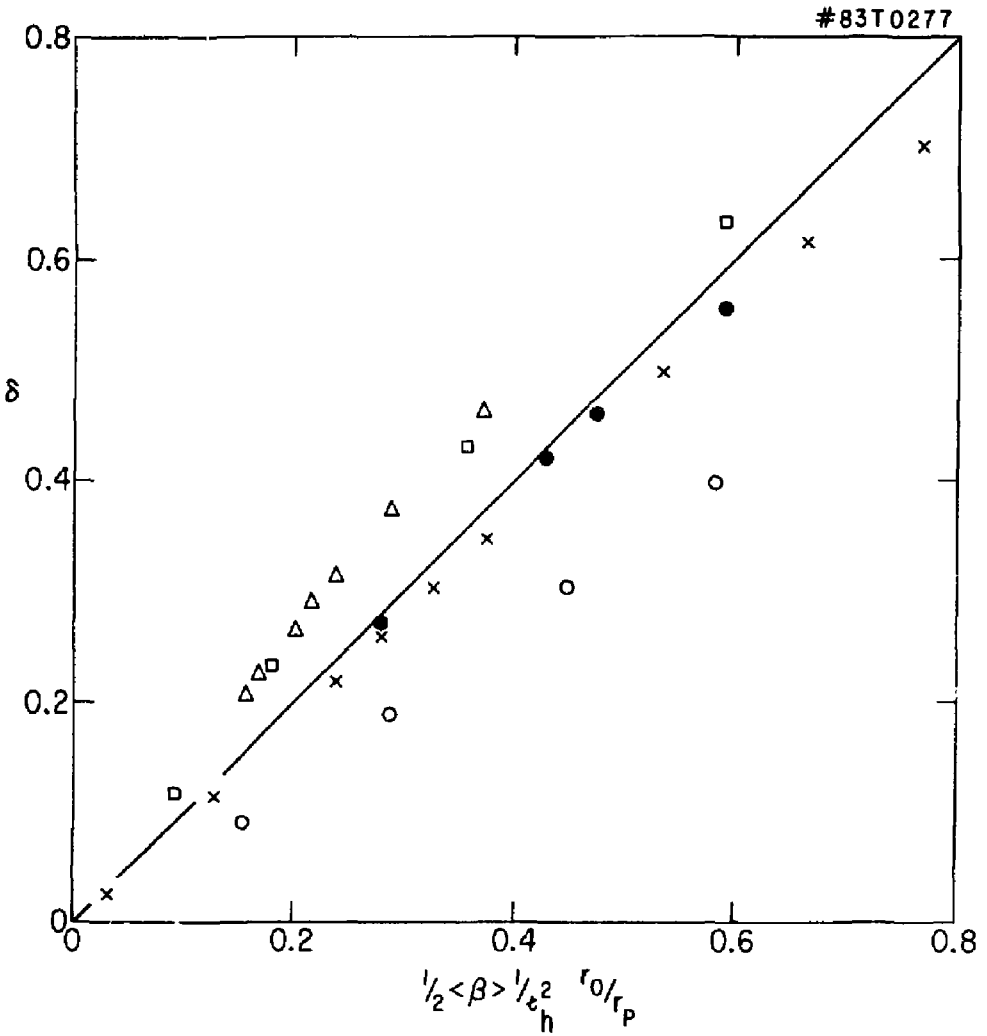
#83T0277
0.8
0.6
0.4
0.2
0
δ
0
0.2
0.4
0.6
0.8
$\frac{1}{2}<\beta>\frac{1}{\epsilon_h^2}\ r_0/r_p$

Fig. 13

EXTERNAL DISTRIBUTION IN ADDITION TO TIC UC-20

Plasma Res Lab, Austra Nat'l Univ, AUSTRALIA
Dr. Frank J. Paoloni, Univ of Wollongong, AUSTRALIA
Prof. I.R. Jones, Flinders Univ., AUSTRALIA
Prof. M.H. Brennan, Univ Sydney, AUSTRALIA
Prof. F. Cap, Inst Theo Phys, AUSTRIA
Prof. Frank Verheest, Inst theoretische, BELGIUM
Dr. D. Palumbo, Dg XII Fusion Prog, BELGIUM
Ecole Royale Militaire, Lab de Phys Plasmas, BELGIUM
Dr. P.H. Sakanaka, Univ Estadual, BRAZIL
Dr. C.R. James, Univ of Alberta, CANADA
Prof. J. Teichmann, Univ of Montreal, CANADA
Dr. H.M. Skarsgard, Univ of Saskatchewan, CANADA
Prof. S.R. Sreenivasan, University of Calgary, CANADA
Prof. Tudor W. Johnston, INRS-Energie, CANADA
Dr. Hannes Barnard, Univ British Columbia, CANADA
Dr. M.P. Bachynski, MPB Technologies, Inc., CANADA
Zhengwu Li, SW Inst Physics, CHINA
Library, Tsing Hua University, CHINA
Librarian, Institute of Physics, CHINA
Inst Plasma Phys, SW Inst Physics, CHINA
Dr. Peter Lukac, Komenskeho Univ, CZECHOSLOVAKIA
The Librarian, Culham Laboratory, ENGLAND
Prof. Schatzman, Observatoire de Nice, FRANCE
J. Radet, CEN-BP6, FRANCE
AM Dupas Library, AM Dupas Library, FRANCE
Dr. Tom Nual, Academy Bibliographic, HONG KONG
Preprint Library, Cent Res Inst Phys, HUNGARY
Dr. A.K. Sundaram, Physical Research Lab, INDIA
Dr. S.K. Trehan, Panjab University, INDIA
Dr. Indra Mohan Lal Das, Banaras Hindu Univ, INDIA
Dr. L.K. Chavda, South Gujarat Univ, INDIA
Dr. R.K. Chhajlani, Var R_chi Marg, INDIA
P. Kaw, Physical Research Lab, INDIA
Dr. Phillip Rosenau, Israel Inst Tech, ISRAEL
Prof. S. Cuperman, Tel Aviv University, ISRAEL
Prof. G. Rostagni, Univ Di Padova, ITALY
Librarian, Int'l Ctr Theo Phys, ITALY
Miss Clelia De Palo, Assoc EURATOM-CNEN, ITALY
Elbiloteca, del CNR EURATOM, ITALY
Dr. H. Yamato, Toshiba Res & Dev, JAPAN
Prof. H. Yoshikawa, JAERI, Tokai Res Est, JAPAN
Prof. T. Uchida, University of Tokyo, JAPAN
Research Info Center, Nagoya University, JAPAN
Prof. Kyoji Nishikawa, Univ of Hiroshima, JAPAN
Prof. Sigeru Mori, JAERI, JAPAN
Library, Kyoto University, JAPAN
Prof. Ichiro Kawakami, Nihon Univ, JAPAN
Prof. Satoshi Itoh, Kyushu University, JAPAN
Tech Info Division, Korea Atomic Energy, KOREA
Dr. R. England, Ciudad Universitaria, MEXICO
Bibliotheek, Fom-Inst Voor Plasma, NETHERLANDS
Prof. B.S. Liley, University of Waikato, NEW ZEALAND
Dr. Suresh C. Sharma, Univ of Calabar, NIGERIA
Prof. J.A.C. Cabral, Inst Superior Tech, PORTUGAL
Dr. Octavian Petrus, ALI CUZA University, ROMANIA
Dr. R. Jones, Nat'l Univ Singapore, SINGAPORE
Prof. M.A. Hellberg, University of Natal, SO AFRICA
Dr. Johan de Villiers, Atomic Energy Bd, SO AFRICA
Dr. J.A. Tegle, JEN, SPAIN
Prof. Hans Wilhelmson, Chalmers Univ Tech, SWEDEN
Dr. Lennart Stenflo, University of UMEA, SWEDEN
Library, Royal Inst Tech, SWEDEN
Dr. Erik T. Karlson, Uppsala Universitet, SWEDEN
Centre de Recherchesen, Ecole Polytech Fed, SWITZERLAND
Dr. W.L. Weise, Nat'l Bur Stand, USA
Dr. W.M. Stacey, Georg Inst Tech, USA
Dr. S.T. Wu, Univ Alabama, USA
Prof. Norman L. Oleson, Univ S Florida, USA
Dr. Benjamin Ma, Iowa State Univ, USA
Prof. Magne Kristiansen, Texas Tech Univ, USA
Dr. Raymond Askew, Auburn Univ, USA
Dr. V.T. Tolok, Kharkov Phys Tech Ins, USSR
Dr. D.D. Ryutov, Siberian Acad Sci, USSR
Dr. M.S. Rabinovich, Lebedev Physical Inst, USSR
Dr. G.A. Eliseev, Kurchatov Institute, USSR
Dr. V.A. Glukhikh, Inst Electro-Physical, USSR
Prof. T.J. Boyd, Univ College N Wales, WALES
Dr. K. Schindler, Ruhr Universitat, W. GERMANY
Nuclear Res Estab, Julich Ltd, W. GERMANY
Librarian, Max-Planck Institut, W. GERMANY
Dr. H.J. Kaeppler, University Stuttgart, W. GERMANY
Bibliothek, Inst Plasmaforschung, W. GERMANY